

RESEARCH

Open Access



The Effect of Rebar Embedment and CFRP Confinement on the Compressive Strength of Low-Strength Concrete

Nima Hashemi¹, Sina Hassanpour^{2*}  and Asghar Vatani Oskoei¹

Abstract

Low-strength concrete (LSC) elements are prone to several seismic and static loads and are one of the priorities to be considered for FRP strengthening. However, certain provisions should be taken into account according to provisions, as elements with considerably low compressive strength are not eligible for FRP confinement. This experimental study investigates (1) the effect of rebar planting on increasing the initial compressive strength of LSC to achieve allowable compressive strength for FRP strengthening, and (2) the effect of CFRP confinement on increasing the strength of rebar-embedded specimens and determining the most effective factor for strength improvement. For this purpose, 38 standard concrete cylinders were tested under compressive load. The variables of this study were rebar length and diameter, the compressive strength of concrete, and the number of CFRP sheets. Two initial compressive strengths below the designated compressive strength of 17 MPa (12.5 and 14.5 MPa) were selected. After determining rebar-reinforced specimens with compressive strength of more than 17 MPa, CFRP confinement and compressive tests of these cylinders were utilized. A statistical single-factor ANOVA analysis is performed to determine the most effective variable for ultimate strength and strain, individually. In the end, available models in the literature were utilized to predict experimental data. The results indicated the effectiveness of rebar planting for strength enhancement up to 53%, also showing that specimens with initial compressive strength of 14.77 MPa were suitable for CFRP confinement after rebar planting. The experimental and statistical ANOVA results demonstrated the CFRP confinement and its interaction with rebar embedment as the most effective factors with respect to increasing the load-bearing capacity of LSC concrete.

Keywords: low-strength concrete (LSC), confinement, CFRP fibers, rebar installation, ANOVA analysis

1 Introduction

Various structures, especially in developing countries require retrofitting. Construction defects, non-compliance of structure with new design regulations, degradation due to environmental factors, and damage from natural disasters are all among the reasons for structural retrofitting requirements (Mosallam, 2004). Along

with these factors, the construction malfunctions such as low quality of used materials and poor construction practices are two main factors affecting the performance and strength of reinforced concrete (RC) structures and intensify the need for rehabilitation and strengthening of structural elements (Durrani et al., 2005; Naseer et al., 2006; Nisikawa et al., 2005; Peiris et al., 2006).

Concrete with a compressive strength between 5 and 15 MPa, has been introduced as a low-strength concrete (LSC) (Ahmad et al., 2015). Low-strength concrete can be used in several sections of buildings and structures where no significant loads are present. Nevertheless, sometimes the creation of low-strength concrete

*Correspondence: sinahassanpour@alum.sharif.edu

² Department of Civil and Environmental Engineering, Sharif University

of Technology, Azadi Ave., Tehran, Iran

Full list of author information is available at the end of the article

ISSN 1976-0485 / eISSN 2234-1315.

members is unintentional or is not based on the design regulations and may create dangerous structural failure conditions. Hyogo-ken-Nanbu earthquake reports that a large number of low-strength concrete with a compressive strength of less than 10 MPa were found in concrete cores from buildings constructed during the 1960s and 1970s (Hiroaki et al., 2008). One of the most reliable methods to strengthen reinforced low-strength concrete elements is the utilization of FRP sheets as confinement (Saeed et al., 2016). High tensile strength and modulus of elasticity, lightweight, and secure handling are some advantages to using the FRP reinforcement technique (Lim & Ozbakkaloglu, 2015). In the last decade, various studies have introduced different methods for increasing the compressive strength and deformability of structural members through confinement by FRP. The results of these studies demonstrate the strength and deformability improvement of specimens reinforced with FRP jackets (Erdil et al., 2008; Lam & Teng, 2004; Nanni & Bradford, 1995; Saafi et al., 1999). The results of utilizing confinement with FRP sheets indicate an improvement in structure bearing capacity and plasticity (Mirmiran & Shahawy, 1997).

The concrete elements are usually confined by a sufficient amount of FRP sheets to obtain a reliable performance. The softening post-peak branch of the stress–strain graph of concrete transforms to a linear ascending branch with a positive slope. A significant increase in compressive strength of confined concrete will increase the flexural capacity of the FRP-confined structural members (Comert et al., 2009).

Compared to the other FRP productions, carbon fibers possess more tensile strength and their unique mechanical features caught the interest of many researchers over the last years, especially for strengthening. For instance, investigating the effect of confinement with CFRP materials on low and medium strength concrete has discovered that extra rigidity will provide for specimens due to confinement (Ilki et al., 2004).

Falayah (Hassan et al., 2016) investigated CFRP-confined low-strength RC columns under concentric loads. The shape and the slenderness of the column, the thickness, and the configuration of confinement were the basic parameters considered in the experimental program. The increase in ultimate load ranges between 15 and 291% compared to the control specimens.

Ilki et al. (2002) investigated the strength and deformability of low-strength concrete confined by CFRP sheets. This study considers 12 low-strength (f'_c : 6 MPa) cylinder specimens under concentric compression which are wrapped by FRP jackets of various thicknesses. Moreover, the experimental results of this study compared with the experimental behavior of low-strength unconfined

concrete and normal strength (f'_c : 20–35 MPa) specimens that were wrapped by FRP jackets of various thicknesses and layers. Ruqayyah Ismail et al., (2019) investigated the effect of confinement with CFRP sheets, and the result shows that confinement of the concrete can enhance the compressive strength of the specimens up to about 70% of their initial compressive strength. Ali Raza et al. (Raza et al., 2021) conducted research on CFRP strengthening of hybrid reinforced LSC concrete in which confining specimens with CFRP layers demonstrated a significant increase in compressive strength. Ahmad et al., (2020) proposed a numerical and Artificial Neural Network method to model CFRP confined RC cylinders and results demonstrated the high accuracy of proposed models to predict experimental observations.

Another approach in strengthening is a method, which is commonly being used for stabilization of soil structures and retaining walls, is named rebar planting or micropile, and has been developed based on the arrangement of nails in the depth of the wall. Nail arrangement is usually achieved through trial and error among layouts that satisfy safety stabilization factors and modifications as nail length decreases from the top to the bottom of the walls. The nails will be capable of resisting tensile stress, shear stress, flexural moment, and the displacement of the soil mass. Rebar installation helps in attaching concrete parts of a structure to new elements (Najafi et al., 2015).

Rebar installation can be implemented into both fresh and dry concrete (Çalışkan et al., 2013; Cook, 1993; Eligehausen et al., 2006; Upadhyaya & Kumar, 2015). During rebar installation, a hole is created on the surface and is filled with a special adhesive, which is usually an epoxy resin or expansive additive cementitious material. This method is convenient and widely applicable because of its easy installation and high flexibility (Upadhyaya & Kumar, 2015). In this system, the effectiveness of planted rebar on concrete is dependent on the bonding between the adhesive and planted rebar and the bonding between concrete and the adhesive (ACI440.2R-08, 2008). Due to the advancements made in polyester, vinyl ester, and a variety of adhesives in the 1990s, rebar installation through chemical adhesives have gradually replaced the planting method with cementations materials (Çalışkan, 2013; Cook, 1993; González, 2018). Chemical adhesives are composed of special polymers with a synthetic silica type. These adhesives contain several characteristics such as very low shrinkage, high resistance to exhaustion, better performance against corrosion, and quick and easy installation (González et al., 2018).

The strengthening of LSC concrete elements was always a challenging factor. According to Clause 1.3.4 of the ACI440.2R-08 (ACI440.2R-08, 2008), FRP materials

should not be used for critical applications when the compressive strength of the concrete is less than 17 MPa. Although LSC strengthening using FRP sheets was performed in the literature (Aslam et al., 2021; Khaloo et al., 2020; Zhai et al., 2021), studies on the methods of increasing the initial compressive strength of LSC concretes to the designated level and meeting the requirements of ACI code are scarce.

As stated earlier, ACI440.2R-08 (Khaloo et al., 2020) prohibits the application of FRP layers on damaged elements or structures with compressive strength less than 17 MPa. Therefore, attempts were made to increase the strength or repair damaged concrete structures using the injection of grout (Aslam et al., 2021). Nevertheless, the preparation and application of grouts can be challenging due to the lack of space to cast fresh grout or resulting in inappropriate surfaces for FRP confinement, subsequently increasing the costs of strengthening. As a result, novel methods should be taken into account to fortify low-strength concretes without experiencing the above-mentioned impediments. Therefore, the aim of this study is to investigate the influence of rebar planting on increasing the compressive strength of low-strength concrete as well as evaluating the CFRP confinement effect on rebar-strengthened specimens. In this experimental study, 38 concrete cylinders with 150 mm in diameter and 300 mm in height with two different compressive strength groups were used. The variables of this study were concrete compressive strength, length and diameter of embedding rebars, and the number of CFRP confinement. The novelty of this research is to enhance the compressive capacity of low-strength concrete cylinders by embedding reinforcing bars to make them allowable for FRP strengthening. In the end, the influence of variables on strength and strain factors is investigated through ANOVA analysis.

2 Material Properties

2.1 Concrete

The concrete mix design was determined after five mixes when the desired low-strength concrete level was achieved. Two mix designs were selected to obtain

Table 1 Concrete mix design and compressive strength of specimens.

Target compressive strength (MPa)	Water (kg/1 m ³)	Cement (kg/1 m ³)	Sand (kg/1 m ³)	Gravel (kg/1 m ³)	W/C
12.5	148	245	531	707	0.46
14.5	153	279	519	694	0.54

target compressive strengths less than 17 MPa (12.5 and 14.5 MPa) in which their corresponding mix design are provided in Table 1.

Three concrete cylinders from each mix design were provided to determine their compressive strength, according to ASTM C39 (ASTM C39/C39M, 2014). The compressive strength of concrete were 14.77 MPa and 12.45 MPa as shown in Table 1. Table 2 presents the average compressive test results of three identical specimens for each mix design.

2.2 Rebar

Steel reinforcement is utilized to plant inside the cylinders. Two rebar lengths (35 and 55 mm) and two rebar diameters (8 and 10 mm) were considered as variable parameters. Table 3 represents the mechanical properties of rebar, which is used in this study.

2.3 Chemical Adhesives

To provide connection and integrity between embedding rebar and concrete, a chemical adhesive was injected into the gap between rebar and concrete. Table 4 shows the mechanical properties of the chemical adhesive determined by the manufacturer. A second chemical adhesive is used for attaching CFRP wraps to the specimens, and its properties are presented in Table 5.

2.4 CFRP Sheets

A unidirectional carbon fiber-reinforced polymer (CFRP) wrap with a thickness of 0.3 mm was utilized to confine the concrete cylinders (Fig. 1). The CFRP can control the lateral strain of the concrete because of its high tensile strength as the compressive load increases. Approximately 50 mm overlap was considered in the confinement of cylinders with CFRP wrappings. Table 6 shows the

Table 2 Concrete characteristics.

Concrete mix number	Axial ultimate strain (mm/mm, %)	Axial cracking strain (mm/mm, %)	Average compressive strength (MPa)
1	0.35	0.22	14.77
2	0.35	0.24	12.45

Table 3 Mechanical properties of rebar.

Rebar diameter (mm)	Yield tensile strength (MPa)	Ultimate tensile strength (MPa)	Modulus of elasticity (GPa)	Axial yield strain (mm/mm, %)
8	340	500	210	1.2×10^{-3}
10	340	500	210	1.2×10^{-3}

Table 4 Mechanical properties of chemical adhesive.

Anchor rod class	Drill diameter (mm)	Embedment depth (mm)	Standard edge distance (mm)	Standard anchor distance (mm)	Torque moment (N m)	Characteristic tensile resistance (kN)
M8	10	80	80	160	10	12.9
M10	12	90	90	180	20	19.7

Table 5 Resin properties.

Density (kg/l)	1.16
Tensile elasticity modulus (GPa)	3.5
Flexural elasticity modulus (GPa)	2.8
Ultimate tensile strength (MPa)	45
Ultimate shear strength (MPa)	21
Compression strength (MPa)	73

**Fig. 1** CFRP sheets for strengthening.**Table 6** CFRP wraps properties.

Tensile elasticity modulus (GPa)	1400
Ultimate tensile strength (MPa)	3800
Ultimate tensile strain (mm/mm, %)	1.2

mechanical properties of the CFRP wraps used in this study.

3 Experimental Procedure

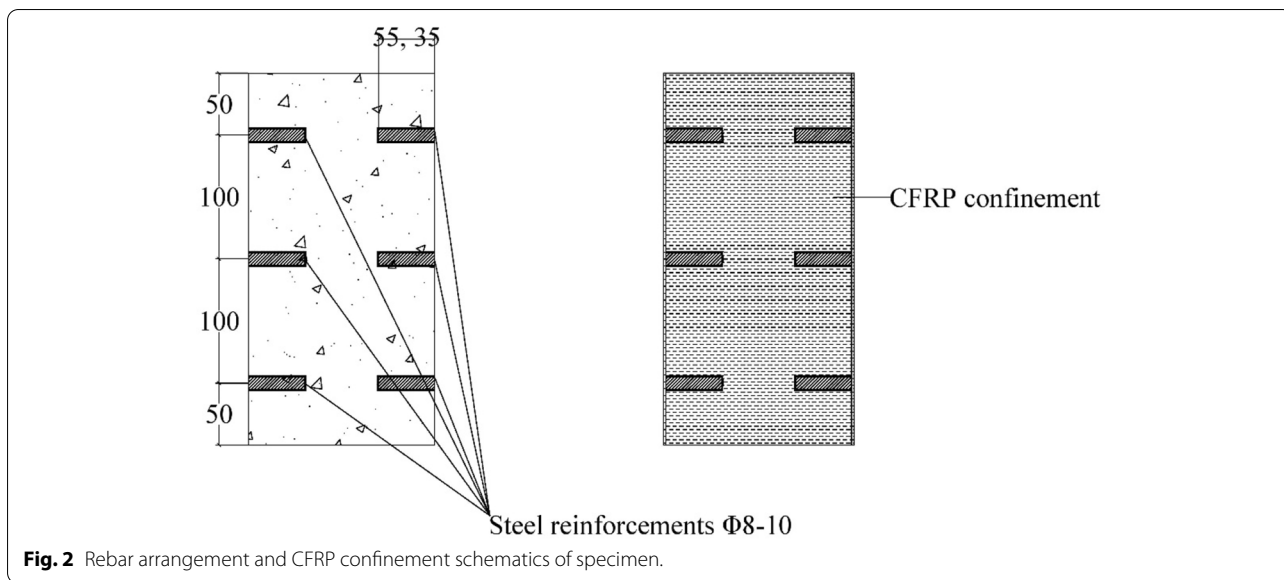
3.1 Rebar Planting in Unconfined Concrete

As mentioned earlier, FRP materials should not be used for critical FRP applications when the compressive strength of the concrete is less than 17 MPa, According

to the ACI440.2R-08 (ACI440.2R-08, 2008). Hence, to exceed the compressive capacity of LSC cylinders, a novel rebar planting method was suggested by the authors to provide the feasibility of FRP confinement for low-strength concrete specimens. Rebar planting was performed according to provisions provided in ACI 318 (ACI 318-14, 2014) and ACI 355.4 (ACI Committee, 2011) to maintain the stability of LSC concrete, as well as the compressive strength enhancement. Similar precautions were taken into the account during tests and based on the results, none of the specimens were damaged during drilling and anchorage procedures. Standard cylindrical low-strength concrete specimens were made to investigate the effect of rebar planting. Designation of specimens is presented as $C_xD_yL_z-t$, where x defines the compressive strength of unconfined concrete, y demonstrates the diameter of planted rebar, z is the length of rebar, and t shows the number of identical specimens, which two duplication for each designation is considered in this study to achieve reliable results. For better clarification, in specimen C14.77D8L3.5, the first part, C14.77, represents the compressive strength of initial concrete, which is 14.77 MPa. The second term, D8, shows the diameter of the rebar planted in a cylinder, which is 8 mm. Finally, the third part, L3.5, indicates the length of the rebar, which equals 3.5 cm. Fig. 2 illustrates the arrangement of rebars and FRP confinement in the cylindrical specimens.

For planting the rebar within the cylindrical specimens, first, holes were drilled with the help of specialists to avoid damage to concrete, and then holes were filled with resin. According to the ACI408R-03 (ACI Committee 355, 2011) regulation, drilled holes length should not be more than half the specimen thickness. As mentioned earlier, the length of rebar is one of the variable parameters in this study. Hence, for 35- and 55-mm-length rebars, 40- and 60-mm-length holes were created in specimens. Five millimeters gap in length provides sufficient space for the adhesive to attain a desirable bond between reinforcements and concrete. Also, the drill size was selected as 2 mm bigger than rebars to allocate space for the adhesive to be functional with respect to maintaining its bond with concrete and steel rebar.

Fig. 3 shows the drilling and rebar planting procedure. The created holes were cleaned to prevent bond strength



decrease due to the presence of dust and powdered concrete. Special rebar planting adhesive was utilized to plant the rebar specimens in concrete afterward.

3.2 CFRP Confinement of Concrete

Four designations of the rebar-planted specimens were considered for CFRP sheet confinement. Since the overall compressive strength of reinforced cylinders with initial concrete strength of 12.45 falls below the minimum strength allowable for FRP utilization (16.86 MPa < 17 MPa), only cylinders with concrete strength of 14.77 MPa were selected for CFRP confinement, according to ACI440.2R-08. It can be mentioned that the designations of confined specimens are almost similar to that of only rebar-planted specimens (Cx Dy Lz-tLC). The only difference is the definition of t, which presents the number of CFRP layers wrapped in each concrete cylinder.

The compressive strength test was performed after specimen preparation. In order to obtain the

stress–strain diagram of specimens, a load cell was used to get the compressive load on the specimens, and two LVDTs were employed to measure the displacement of the specimens. Same as the previous setup, two identical specimens were prepared to verify the results. Fig. 4 shows the placement position of LVDTs and load cells with corresponding schematics, by which the rebar strain is measured with a strain gauge. Two LVDTs are placed on top of the loading cell to measure the vertical displacement of specimens, while strain gauges are placed on rebars to measure the deformation.

4 Test Results

4.1 Effect of Rebar Planting

Compressive strength test results on specimens are shown in Table 7. The results indicate that planting rebar within the low-strength concrete increases the compressive strength of concrete. The maximum and minimum strength increase ratio belongs to specimens C14.77D10L5.5 and C12.45D8L3.5, with 53% and 30%

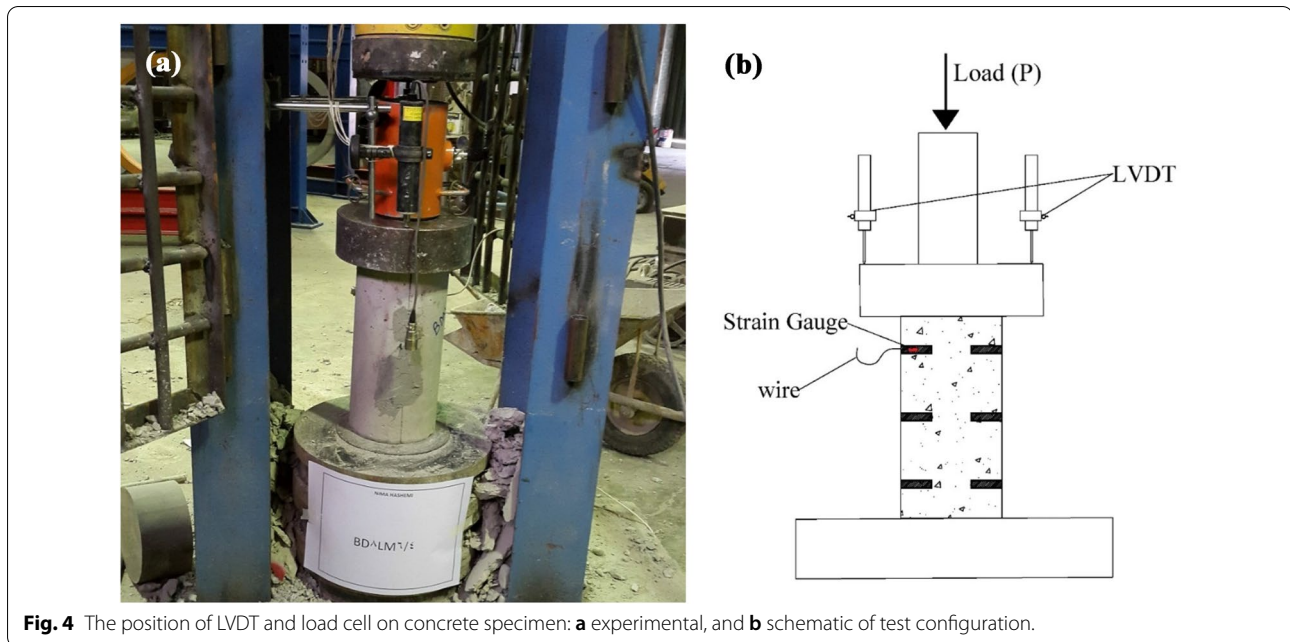


Fig. 4 The position of LVDT and load cell on concrete specimen: **a** experimental, and **b** schematic of test configuration.

Table 7 Compressive strength test results of specimens embedded with steel reinforcement.

Specimen name	Compressive strength (MPa)	Specimen compressive strength at rebar slip (MPa)	The final output of rebar from the concrete body (mm)	Axial cracking strain (mm/mm, %)	Maximum of rebar axial strain (μ strain)	Axial ultimate strain (mm/mm, %)	Average of compressive strength (MPa)
C14.77D8L3.5-1	19.57	19.42	2.5	0.26	–	0.37	19.55
C14.77D8L3.5-2	19.53	19.12	3	0.24	650.7	0.36	
C14.77D8L5.5-1	19.91	19.51	4	0.29	–	0.38	19.88
C14.77D8L5.5-2	19.86	18.76	4	0.3	753.4	0.39	
C14.77D10L3.5-1	21.77	21.41	1.5	0.32	–	0.39	21.53
C14.77D10L3.5-2	21.29	21.01	1	0.33	536.5	0.4	
C14.77D10L5.5-1	22.65	21.66	1.5	0.32	–	0.42	22.61
C14.77D10L5.5-2	22.57	21.70	1	0.33	536.5	0.41	
C12.45D8L3.5-1	15.88	15.27	3	0.23	–	0.31	16.24
C12.45D8L3.5-2	16.21	15.61	2.5	0.21	519.5	0.33	
C12.45D8L5.5-1	16.73	16.21	4	0.29	–	0.38	17.08
C12.45D8L5.5-2	17.06	16.56	4	0.31	572.5	0.39	
C12.45D10L3.5-1	17.18	16.63	2	0.32	–	0.35	17.16
C12.45D10L3.5-2	17.14	16.58	2.5	0.3	395.7	0.36	
C12.45D10L5.5-1	17.36	16.90	1.8	0.33	–	0.34	17.28
C12.45D10L5.5-2	17.25	16.74	2.2	0.29	343.2	0.32	

increment in compressive strength capacity, respectively. Based on the results, increasing the bar diameter increased the ultimate strength of the specimen after rebar embedment. Moreover, the embedment length of planted rebars has shown a positive effect on the compressive strength, as in the specimen with concrete strength of 14.77 MPa, 5%, and in the specimens with

concrete strength of 12.45 MPa, a 7% increase in compressive strength was observed. Generally, test results demonstrate that the compressive strength of concrete slightly contributes to the effectiveness of confinement and rebar planting, where utilizing concrete with higher strength, increases the influence of strengthening.

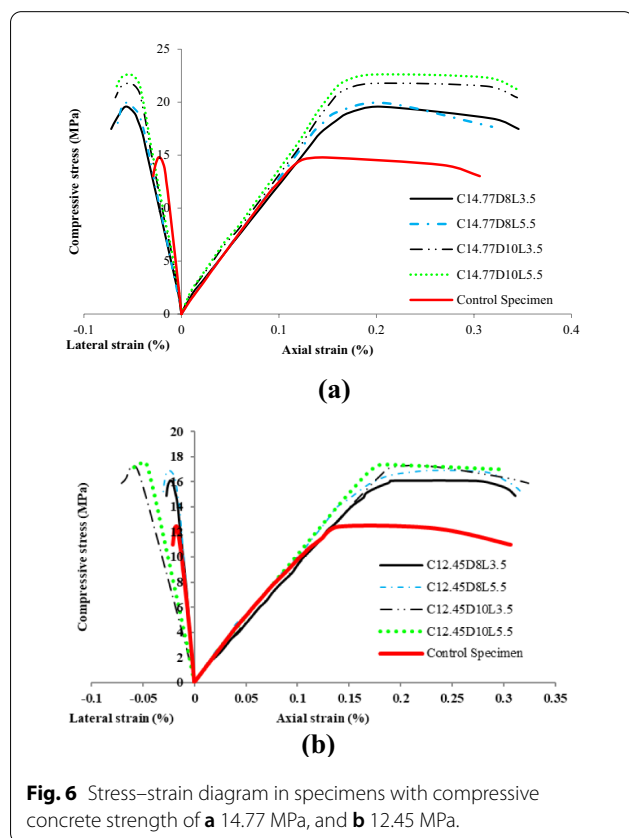
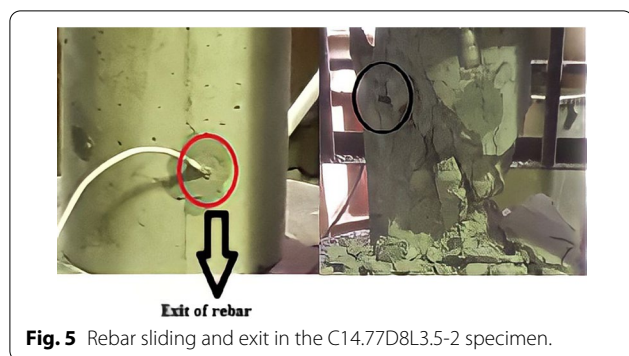


Fig. 5 shows the rebar sliding in the C14.77D8L3.5 specimen during and after the test. Before the failure of specimens, planted rebars inside concrete experienced 1 to 5 mm slippage. This was followed by the reduction in load-bearing capacity of cylinders and consequently reaching the failure state. Moreover, comparing the stress–strain diagrams of each specimen shows that the axial and lateral strain in the initial specimens increased due to rebar planting; Fig. 6 demonstrates strain–stress diagrams of specimens with rebar, and they compared with the stress–strain diagram of the average of three initial specimens without rebar. According to the diagrams,

embedding the rebar into low-strength concrete is effective in increasing the compressive strength of the concrete. According to the results, the influence of rebar planting on increasing the axial strain is slight. However, the increase in lateral strain is considerable.

As stated in the Introduction, despite several studies on FRP confinement of LSC concrete, there are few research articles available that studied the increasing the initial strength of LSC to make FRP strengthening applicable, with respect to provisions of ACI 440.2R (ACI440.2R-08, 2008). Although using grout is recommended for some cases, it produces disadvantages such as unsmooth surface after grouting and increasing the cost of strengthening, challenges of casting grout due to lack of space and postpone in the process of strengthening due to the curing process of grout. Therefore, the proposed method can be utilized with considering provisions for application, as stated in ACI 318 (ACI 318-14, 2014) and ACI 355.4 (ACI Committee, 2014) to satisfy the compressive strength requirement, per ACI 440.2R (ACI440.2R-08, 2008).

4.2 Effect of CFRP Confinement

The compressive strength test was carried out first on the unconfined specimens. After determining the valid specimens for CFRP strengthening (compressive strength of 14.77 MPa), after confining corresponding cylinders, compressive strength test is performed. A total of 16 specimens were tested. Table 8 presents the test results of the compressive strength of confined specimens. The compressive strength test results show that rebar planting with confinement increased the compressive strength of specimens around 200% of the initial cylinders. The ultimate strain also experienced an increase due to the confinement effect of CFRP sheets.

The minimum and maximum strength increase were observed in specimens “C14.77D8L5.5-1LC” and “C14.77D10L5.5-2LC”, with a rate of 84.2 and 161.34% increase to initial strength of 14.77 MPa, respectively. Results also indicate that the addition of a second CFRP layer contributes to ultimate strength 47% on average.

Figs. 7 and 8 show test setup of confined specimens and a specimen under a compressive strength test after failure, respectively. Due to the increment in compressive stress applied by the hydraulic jack, bulging as the result of lateral expansion in cylinders was observed. Therefore, the failure occurred due to an increase in lateral deformation in core concrete and subsequently, rupturing confining CFRP sheets.

Fig. 9 shows the strain–stress diagram of confined specimens and unconfined specimens with and without rebar in a comparative manner. Although rebar embedment demonstrated a remarkable increase of

Table 8 Compressive strength of each specimen confined with CFRP fibers.

Specimen name	Experimental compressive strength of confined specimen (MPa)	Ultimate axial strain (mm/mm, %)	Average compressive strength in unconfined specimens with rebar embedment (MPa)	Average compressive strength of confined specimens (MPa)
C14.77D8L3.5-1LC-1	27.2	0.46	19.55	27.65
C14.77D8L3.5-1LC-2	28.1	0.48		
C14.77D8L3.5-2LC-1	33.7	0.54	19.55	33.75
C14.77D8L3.5-2LC-2	33.8	0.53		
C14.77D8L5.5-1LC-1	27.0	0.42	19.88	27.3
C14.77D8L5.5-1LC-2	27.6	0.47		
C14.77D8L5.5-2LC-1	34.1	0.57	19.88	34.1
C14.77D8L5.5-2LC-2	34.0	0.58		
C14.77D10L3.5-1LC-1	29.6	0.48	21.53	30.4
C14.77D10L3.5-1LC-2	31.1	0.53		
C14.77D10L3.5-2LC-1	37.1	0.59	21.53	37.15
C14.77D10L3.5-2LC-2	37.2	0.59		
C14.77D10L5.5-1LC-1	31.7	0.56	21.68	31.6
C14.77D10L5.5-1LC-2	31.5	0.54		
C14.77D10L5.5-2LC-1	38.3	0.53	21.68	38.6
C14.77D10L5.5-2LC-2	38.9	0.61		



Fig. 7 CFRP fibers and confined specimens ready for testing compressive strength.

compressive strength in specimens, the effect of confinement on load-bearing capacity is the most significant, and a slight influence on the axial ultimate strain can be observed. Additionally, the CFRP confinement demonstrated a small contribution to the improvement of lateral strain in cylinders. This can be attributed to the lateral resistance of carbon fibers that although contributing to the increment in the strength of specimens, limits the lateral bulging of core concrete until the rupture of CFRP layers.

5 Analysis of the Force–Deformation Diagram of Rebar

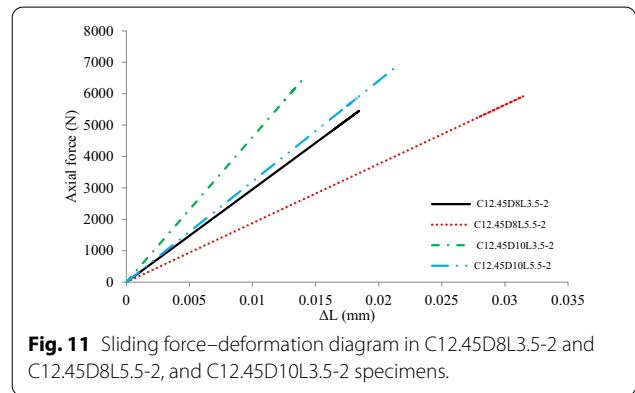
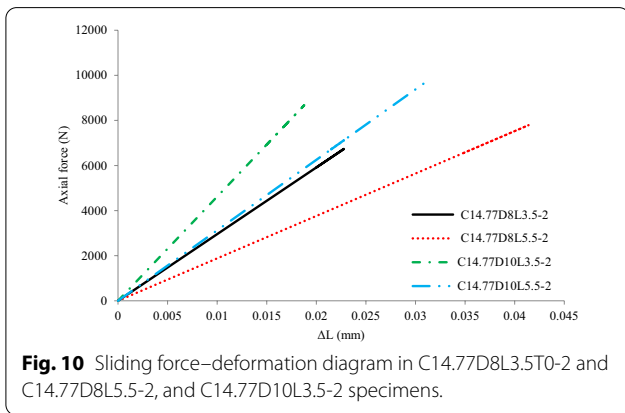
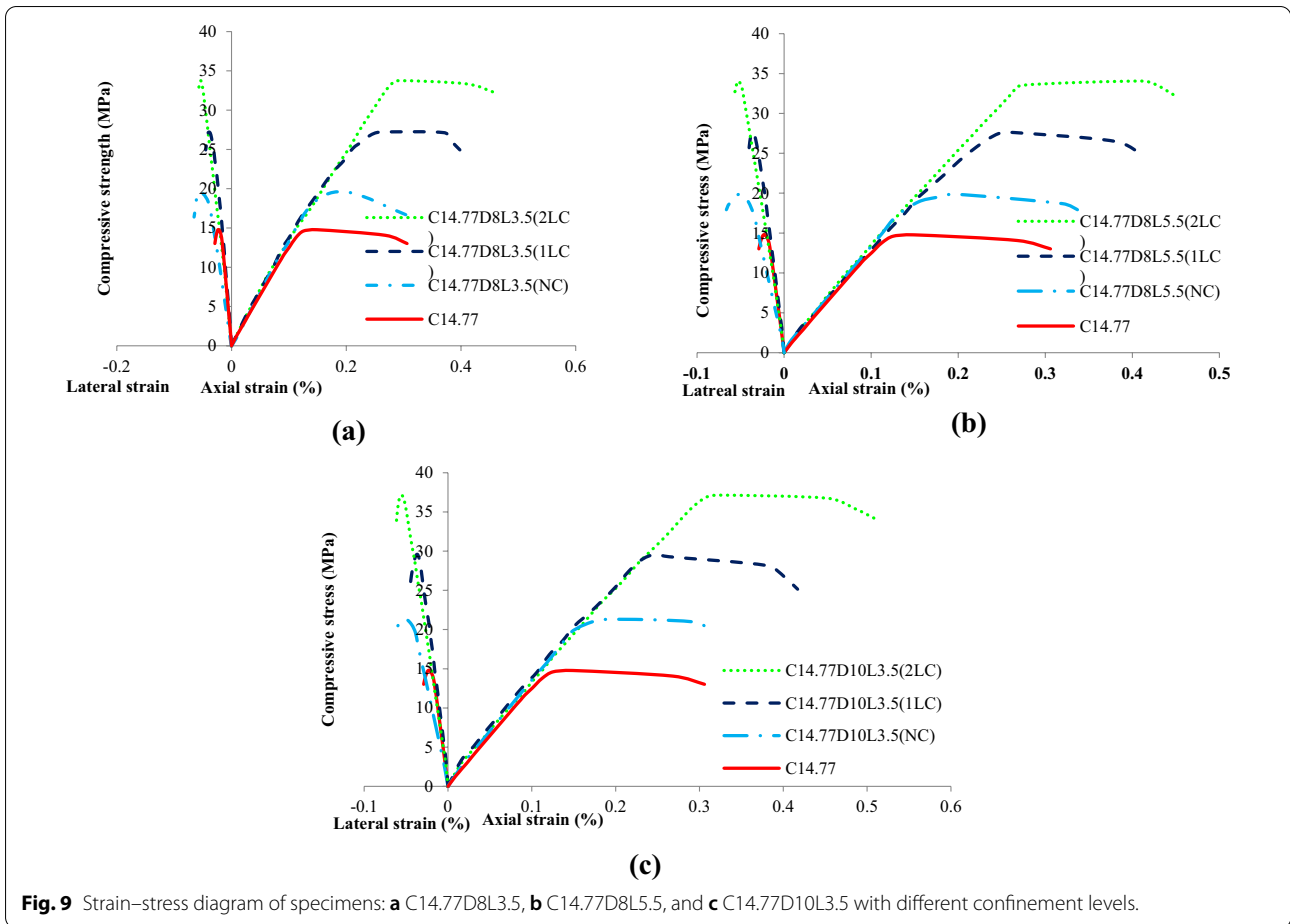
According to the failure mechanism of specimens under the compressive load, the rebar, which is embedded in the concrete specimen slipped from the concrete body. The longitudinal strain of the rebar was measured during loading by strain gauges. Fig. 10 demonstrates the slip force–deformation diagram of embedded rebar in three specimens C14.77D8L3.5-2, C14.77D8L5.5-2, and C14.77D10L3.5. According to the equation of equilibrium, rebar slip force (or bond force) is equal to the axial force of embedded bars. Hence, Hooke’s law is utilized to calculate slip force:

$$F_s = K \Delta l, \tag{1}$$

where F_s is slip force and Δl is deformation of steel bars obtained from strain gauge data. K is the axial stiffness of steel reinforcement and is calculated as follows:



Fig. 8 Confined specimen with embedded rebar after failure.



$$K = \frac{AE}{l_e} \tag{2}$$

In this equation, E is the modulus of elasticity of steel, and A and l_e are cross-sectional area and embedment length of steel rebars, respectively.

The comparison between results of slip force revealed that an increment in rebar diameter increases the slip force generated between rebar and concrete. It attributes to the improvement of axial stiffness as shown in Eq. (2), which consequently increases the slip force. The same trend can also be observed in Fig. 11.

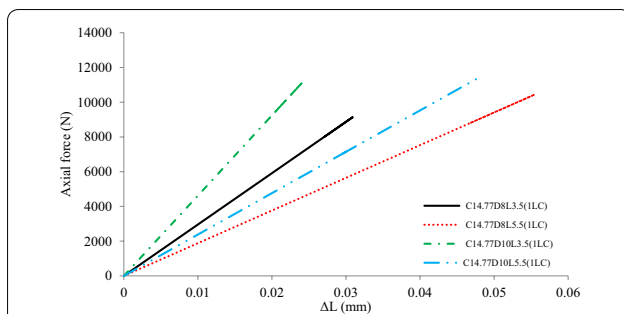


Fig. 12 Sliding force–deformation diagram in C14.77D8L3.5-1LC-2 and C14.77D8L5.5-1LC-2, and C14.77D10L3.5-1LC-2 specimens.

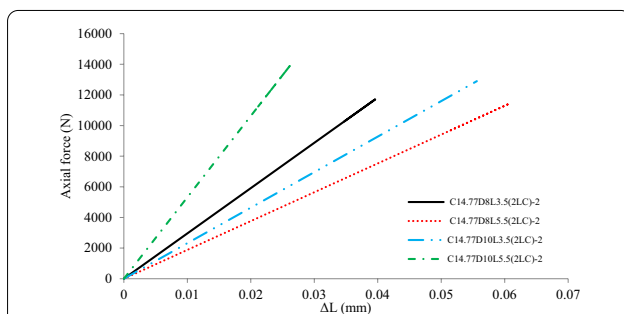


Fig. 13 Sliding force–deformation diagram in C14.77D8L3.5-2LC-2 and C14.77D8L5.5-2LC-2, and C14.77D10L3.5-2LC-2 specimens.

The comparison between Figs. 10 and 12 shows that in confined specimens, the slip force is higher than that of unconfined specimens, also by increasing the rebar stiffness, the slip force increased. Fig. 13 demonstrates that in specimens with two-layer confinement, the slip force and rebar deformation are higher than specimens with one-layer confinement. This indicates that confinement effect controls the rebar slippage by controlling the lateral deformation of core concrete. Table 9 presents the information about the sliding force of the rebar and the longitudinal strain of the rebar in each specimen.

6 ANOVA Analysis

In order to determine the statistical significance of each experimental variable on enhancing strength and strain values, single-factor ANOVA analysis was performed on specimens to determine the contribution of each variable in the improvement of compressive strength and ultimate strain of specimens. ANOVA aims to evaluate the significance of differences between reported results in a statistical manner. The parameter is considered significant when its p -value is under the significance factor of $\alpha=0.05$. Therefore, the smaller the p -value is, the more significant is the corresponding parameter (ACI, 2003). The objective of performing single-factor ANOVA for this study is to a statistical assessment of the significance

Table 9 Maximum force and rebar deformation in different specimens.

Specimen name	Rebar maximum slip force (N)	Rebar maximum deformation ($\times 10^{-5}$ mm)
C14.77D8L3.5-2	6735.3	2277.6
C14.77D8L5.5-2	7798	4143.92
C14.77D10L3.5-2	8676.4	1877.8
C14.77D10L5.5-2	9865.16	3155.6
C12.45D8L3.5-2	5454.4	1844.5
C12.45D8L5.5-2	5926	3149
C12.45D10L3.5-2	6400.1	1385.1
C12.45D10L5.5-2	6891.4	2147.7
C14.77D8L3.5-1LC-2	9139	3091.5
C14.77D8L5.5-1LC-2	10444.5	5550.2
C14.77D10L3.5-1LC-2	11248.05	2434.3
C14.77D10L5.5-1LC-2	11522.1	4850.2
C14.77D8L3.5-2LC-2	11709.8	3959.8
C14.77D8L3.5-2LC-2	11430.7	6074.3
C14.77D8L3.5-2LC-2	12245.9	2650.3
C14.77D8L5.5-2LC-2	12897.9	5516.4

of the variables (i.e., rebar embedment and a number of CFRP layers) in affecting each strength and strain outcome, individually.

The results for each variable are demonstrated in Tables 10 and 11. As it can be observed from the results, the p -value for the rebar embedment is more than 0.05 for both compressive strength and ultimate strain, indicating the insignificance of the variable at increasing both factors compared to other parameters. The least recorded p -values belong to the number of CFRP confinement, which also has the highest contribution percentage of 52.61 and 48.89 for ultimate strength and strain, respectively. This indicates the highest effect of CFRP wrapping on enhancing both load-bearing capacity and deformability of specimens. The interaction between pairs of variables was also investigated and significance is observed among them. This may indicate the importance of rebar planting in confined specimens.

7 Verification of Test Results

In order to predict the compressive strength capacity of the confined concrete, many studies have been performed and different relationships were introduced (Lam & Teng, 2003; Luca & Nanni, 2011; Pham & Hadi, 2014a, 2014b; Pham et al., 2015; Pour et al., 2018; Saeed et al., 2016; St & Wold, 1989; Teng et al., 2009; Wu & Zhou, 2010). The confinement mechanism of FRP-confined concrete for both conditions comprises full and partial confinement presented by Pham et al. (Luca & Nanni,

Table 10 ANOVA analysis results for compressive strength.

Control factor	p-value	Sum of square	Contribution (%)
Rebar size	0.000461	69.11	15.25
Rebar embedment length	0.496024	12.47	2.75
Number of layers	0.000023	238.37	52.61
Interaction of rebar size and embedment length	0.041354	24.93	5.50
Interaction of rebar size and number of layers	0.010593	16.45	3.63
Interaction of rebar embedment and number of layers	0.000111	91.80	20.26

Table 11 ANOVA analysis for ultimate strain.

Control factor	p-value	Sum of square	Contribution (%)
Rebar size	0.01669	0.018	20.00
Rebar embedment length	0.17231	0.003	3.33
Number of layers	0.00198	0.044	48.89
Interaction of rebar size and embedment	0.05088	0.007	7.78
Interaction of rebar size and number of layers	0.04895	0.008	8.89
Interaction of rebar embedment and number of layers	0.03769	0.010	11.11

Table 12 Models for prediction of compressive strength after confinement.

Model	Compressive strength after confinement (MPa)
ACI 440-2R (ACI440.2R-08, 2008)	$f'_{cc} = f'_{co} + 3.3\psi \kappa_a f_t$ $f_t = \frac{2Eftf\epsilon_{fe}}{D}$ $\epsilon_{fe} = \kappa_\epsilon \epsilon_{fu}$
Lam and Teng (Pham & Hadi, 2014b)	$\frac{f'_{cc}}{f'_{co}} = 1 + 3.3 \frac{fl}{r'_{co}}$ $fl = \frac{2Eft\epsilon_{fe}}{D}$
Ali fallahpour et al. (Wu & Zhou, 2010)	$f'_{cc} = f'_{co} + k_1 k_2 \epsilon_{fu}$ $k_1 = 2.5 - 0.01f'_{co}$ $k_2 = \frac{2Eftf}{D}$
Richart et al. (Pour et al., 2018)	$f'_{cc} = f'_{co} + k_1 f_r$ $f_r = \frac{2f_{ij}}{D}$

2011). Due to the originality of the rebar planting method and lack of models considering the effect of steel rebars in LSC concrete, the selection of these models for verification was performed to cover the most notable models in the literature to provide a comprehensive assessment of the comparison.

Table 12 shows different equations available for modeling the effect of CFRP confinement (Ilki et al., 2004; Luca & Nanni, 2011; Pham et al., 2015; Saeed et al., 2016).

shows different equations available for modeling the effect of CFRP confinement (ACI440.2R-08, 2008; Pour, 2018; Richart, 1928; Teng, 2009). As a result of novelty in the proposed method, in these equations, the effect of the embedded rebar is not considered. The definition of variables is presented in Appendix 1

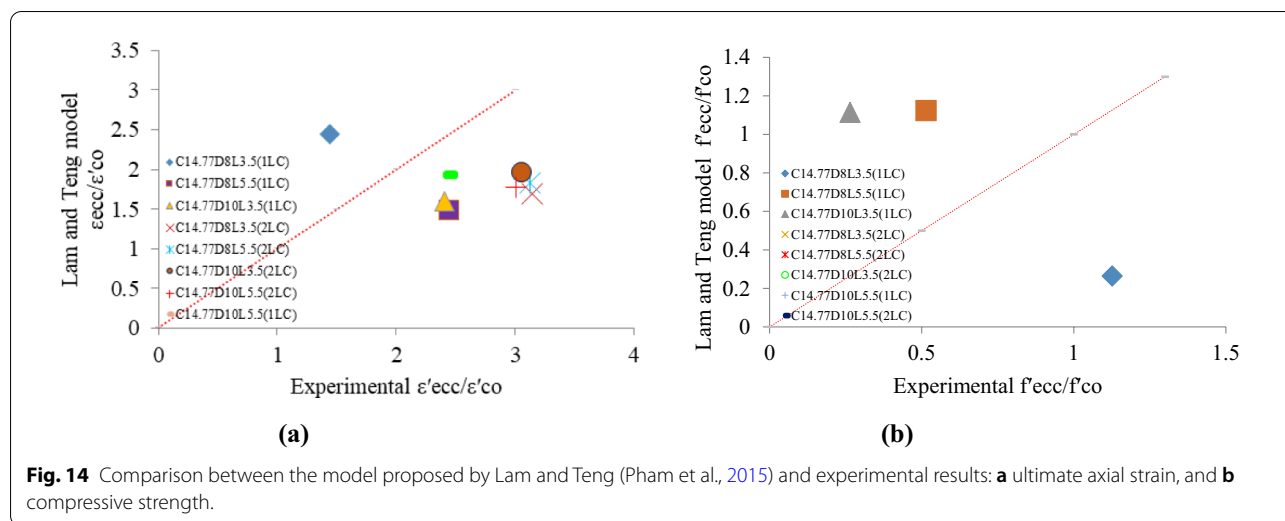
The estimation of compressive strength by each model is presented in Table 13. All models underestimated the compressive strength of cylinders. The ratio of calculated compressive strength to experimental results was around 1.30 for all models. The discrepancy between models and actual data is attributed to the involvement of embedded bars' influence on experimental results. However, the models show proper correlation with experimental data, with the maximum R2 value of 0.97 for Richart et al. (1928) and a minimum of 0.95 for ACI 440-2R (ACI440.2R-08, 2008) models. The experimental model is also compared with the model proposed by Lam and Teng (Pham & Hadi, 2014b) in terms of ultimate axial strain and compressive strength (Fig. 14). The model was unable to predict ultimate strain as the R2 value of variables was 0.27, however, it demonstrated a good performance in estimating compressive strength, with an R2 value of 0.92. For the better clarification of models accuracy to predict the compressive strength of confined specimens, mean square error (MSE) and average absolute error (AAE) values are calculated using the following equations, respectively (Khaloo et al., 2020):

Table 13 Theoretical compressive strength for each specimen according to models.

(a)												
Rechart et al. (Pour et al., 2018)	f_{ecc} (MPa)	f'_{cc} (MPa)	f'_{co} (MPa)	k_1	f_r (MPa)	f_j (MPa)	f_{ecc}/f'_{cc}	MSE	AAE			
C14.77D8L3.5 (1LC)	27.65	22.61	19.55	4.1	0.74704	186.76	1.23	178.7	1.37			
C14.77D8L5.5 (1LC)	27.30	22.94	19.88		0.74704	186.76	1.19					
C14.77D10L3.5 (1LC)	30.32	24.59	21.53		0.74704	186.76	1.23					
C14.77D10L5.5 (1LC)	31.64	25.52	21.68		0.74704	186.76	1.24					
C14.77D8L3.5 (2LC)	33.71	25.67	19.55		1.49408	186.76	1.31					
C14.77D8L5.5 (2LC)	34.10	26.00	19.88		1.49408	186.76	1.31					
C14.77D10L3.5 (2LC)	37.15	27.65	21.53		1.49408	186.76	1.34					
C14.77D10L5.5 (2LC)	38.62	28.11	21.68		1.49408	186.76	1.41					
Lam and Teng (Pham & Hadi, 2014b)	f_{ecc} (MPa)	f'_{cc} (MPa)	f'_{co} (MPa)	f_1 (MPa)	E_f (KN/mm ²)	ϵ_{fe}	f_{ecc}/f'_{cc}	MSE	AAE			
C14.77D8L3.5 (1LC)	27.65	22.01	19.55	0.75	230	0.812	1.24	109.2	1.07			
C14.77D8L5.5 (1LC)	27.30	22.34	19.88		230	0.812	1.24					
C14.77D10L3.5 (1LC)	30.32	23.99	21.53		230	0.812	1.23					
C14.77D10L5.5 (1LC)	31.64	24.14	21.68		230	0.812	1.31					
C14.77D8L3.5 (2LC)	33.71	24.48	19.55	1.49	230	0.812	1.38					
C14.77D8L5.5 (2LC)	34.10	24.81	19.88		230	0.812	1.37					
C14.77D10L3.5 (2LC)	37.15	26.46	21.53		230	0.812	1.40					
C14.77D10L5.5 (2LC)	38.62	26.61	21.68		230	0.812	1.45					
Ali Fallahpour et al. (Wu & Zhou, 2010)	f_{ecc} (MPa)	f'_{cc} (MPa)	f'_{co} (MPa)	K_1	E_f (kN/mm ²)	ϵ_{fu}	k_1	f_{ecc}/f'_{cc}	MSE	AAE		
C14.77D8L3.5 (1LC)	27.65	22.52	19.55	2.3045	230	1.4	0.92	1.23	166.8	1.32		
C14.77D8L5.5 (1LC)	27.30	22.84	19.88	2.3012	230	1.4	0.92	1.19				
C14.77D10L3.5 (1LC)	30.32	24.47	21.53	2.2847	230	1.4	0.92	1.24				
C14.77D10L5.5 (1LC)	31.64	25.25	21.68	2.2718	230	1.4	0.92	1.25				
C14.77D8L3.5 (2LC)	33.71	25.49	19.55	2.3045	230	1.4	1.84	1.32				
C14.77D8L5.5 (2LC)	34.10	25.81	19.88	2.3012	230	1.4	1.84	1.32				
C14.77D10L3.5 (2LC)	37.15	27.41	21.53	2.2847	230	1.4	1.84	1.36				
C14.77D10L5.5 (2LC)	38.62	28.02	21.68	2.2718	230	1.4	1.84	1.38				
(b)												
ACI 440.2R (ACI440.2R-08, 2008)	f_{ecc} (MPa)	f'_{cc} (MPa)	f'_{co} (MPa)	Ψ	E_f (kN/mm ²)	f_t (MPa)	κ_a	ϵ_{fe}	κ_ϵ	f_{ecc}/f'_{cc}	MSE	AAE
C14.77D8L3.5 (1LC)	27.65	21.89	19.55	0.95	230	0.74704	1	0.812	0.58	1.26	544.5	3.37
C14.77D8L5.5 (1LC)	27.30	22.22	19.88	0.95	230		1	0.812	0.58	1.23		
C14.77D10L3.5 (1LC)	30.32	23.87	21.53	0.95	230		1	0.812	0.58	1.25		
C14.77D10L5.5 (1LC)	31.64	24.16	21.68	0.95	230		1	0.812	0.58	1.31		
C14.77D8L3.5 (2LC)	33.71	24.23	19.55	0.95	230	1.49408	1	0.812	0.58	1.39		
C14.77D8L5.5 (2LC)	34.10	24.56	19.88	0.95	230		1	0.812	0.58	1.39		
C14.77D10L3.5 (2LC)	37.15	26.21	21.53	0.95	230		1	0.812	0.58	1.42		
C14.77D10L5.5 (2LC)	38.62	27.35	21.68	0.95	230		1	0.812	0.58	1.41		

$$MSE = \frac{1}{N} \sum_{i=1}^N (\text{model}_i - \text{experimental}_i)^2. \quad (3)$$

$$AAE = \frac{1}{N} \sum_{i=1}^N \left| \frac{\text{model}_i - \text{experimental}_i}{\text{experimental}_i} \right|. \quad (4)$$



Results of statistical analysis for models are shown in Table 13. The lower values for MSE and AAE indicate the higher accuracy of the model. Therefore, the model proposed by Lam and Teng (Pham & Hadi, 2014b) has the highest, and the ACI model has the lowest accuracy in terms of predicting experimental results. However, due to the novelty of the proposed method, available models could not anticipate the effect of rebar embedment on compressive strength. Yet these models can predict the effect of CFRP confinement on cylinders and provide benchmarks to determine the difference between analytical and experimental results due to the presence of rebar embedment. In addition, using statistical approaches on

these models and experiments helps to demonstrate the most compatible model with test results. This would help future studies in terms of detecting the most appropriate model and revising it for analytic studies of rebar-embedded LSC concrete.

Table 14 demonstrates the comparison between experimental results and the experiments of Hafiz zain Saeid et al. (ACI Committee, 2014) with one layer of confinement, and also their difference with results obtained by ACI440-2R (ACI440.2R-08, 2008) models. The ACI model underestimated the experimental results of the research; nevertheless, it overestimated the results of Hafiz zain Saeid et al. (Pham et al., 2015).

Table 14 Comparison between test results and Hafiz Zain Saeid et al. (Pham et al., 2015) study according to ACI relationships.

Specimen	Initial compressive strength (MPa)	ACI (MPa)	Experimental result (MPa)	Experimental result/initial compressive strength	Experimental result/ACI
C14.77D8L3.5/(1LC)	14.77	21.89	27.2	1.84	1.24
C14.77D8L5.5/(1LC)	14.77	22.22	27.6	1.87	1.24
C14.77D10L3.5/(1LC)	14.77	23.87	29.6	2	1.24
C14.77D10L5.5/(1LC)	14.77	24.59	31.6	2.14	1.29
Hafiz zain saeid (et al.) (ACI Committee, 2014) specimen with one-layer confinement	16.55	32.05	26.48	1.6	0.83
C14.77D8L3.5/(2LC)	14.77	28.91	33.75	2.28	1.17
C14.77D8L5.5/(2LC)	14.77	29.24	34.06	2.31	1.16
C14.77D10L3.5/(2LC)	14.77	30.89	37.15	2.51	1.2
C14.77D10L5.5/(2LC)	14.77	32.16	38.6	2.61	1.2
Hafiz zain saeid et al. (ACI Committee, 2014) specimen with 2 layers confinement	16.55	47.55	34.8	2.1	0.73

8 Conclusion

This study investigated the effect of a novel strengthening method using steel rebar embedment and CFRP confinement on LSC concrete. According to the results of the research, the following conclusions have resulted:

1. Utilizing steel rebars to embed into LSC concrete is an effective and efficient method to increase the initial compressive strength of concrete, since the maximum and minimum of 53% and 30% strength enhancement were observed, respectively. The increase in compressive strength can be mostly attributed to the axial stiffness enhancement of concrete due to the presence of steel.
2. Low-strength concretes with compressive strength of 12.45 MPa and under are not suitable to be considered for FRP confinement, as their compressive strength regarding rebar embedment falls below the minimum considered by ACI 440.2R provision (ACI440.2R-08, 2008). However, the utilization of steel bars to enhance the initial compressive strength of LSC concrete to be considered for CFRP strengthening has been proven to be effective for compressive strength of 14.77 MPa or higher.
3. According to the ANOVA analysis of results obtained from experimental tests, the variation in the number of CFRP layers is the most effective approach to enhance the compressive strength and ultimate strain of concrete with a percentage contribution of 52.61 and 48.89 for ultimate strength and strain, respectively.
4. Despite being effective in enhancing the initial compressive strength of specimens, the rebar embedment has shown less significance compared to CFRP wrapping, as the p -values were more than 0.05 for both ultimate strength and strain. However, rebar size and interaction of rebar embedment and number of layers are significant according to the analysis.
5. The statistical MSE and AAE analyses indicate that despite the presence of a discrepancy between models and experimental data due to the rebar embedment effect, the model proposed by Lam and Teng provides a better correlation with test results compared to other models.

9 Suggestions for Future Work

Considering the effectiveness of rebar embedment in compressive strength enhancement, the authors suggest utilizing the number of embedment rebars as a parameter in LSC concrete to increase the strength of LSC elements with a load-bearing capacity of less than 14.5 MPa.

The various types of FRP confinement can also be utilized in future research. In addition, regarding the comparison between experimental data and models, authors encourage researchers to study recent models, while proposing a model to predict the effect of rebar embedment in FRP-confined LSC cylinders.

Appendix 1

f'_{cc} : Compressive strength of confined concrete psi (MPa).

f'_c : Specified compressive strength of concrete, psi (MPa).

ψ_f : FRP strength reduction factor and it is equal to 0.95 for full wrapped sections.

κ_a : Efficiency factor for FRP reinforcement in determination of f'_{cc} (based on geometry of cross-section) can be taken as 1 for circular cross-sections.

f_1 : Maximum confining pressure due to FRP jacket, psi (MPa).

E_f : Tensile modulus of elasticity of FRP, psi (MPa).

t_f : Nominal thickness of one ply of FRP reinforcement, in. (mm).

ϵ_{fe} : Effective strain level in FRP reinforcement.

D : The diameter of specimen, (mm).

κ_ϵ : Efficiency factor equal to 0.58 for FRP strain to account for the difference between observed rupture strain in confinement and rupture strain determined from tensile tests.

ϵ_{fu} : Design rupture strain of FRP reinforcement, in./in. (mm/mm) equal to 1.4 for CFRP sheets which are used in this research.

k_1 : Lateral stiffness of FRP jacket (MPa).

In the model which is represented by Ali Fallah pour et al. k_1 is compressive strength enhancement coefficient, k_1 in Rechart et al.'s model is confinement ratio that is suggested $k_1 = 4.1$ and also f_r is confining pressure.

Acknowledgements

The authors would like to honor the memory of Dr. Oskoei, who sadly passed away recently, for his supervision, as this work would not be complete without his efforts.

Authors' contributions

NH: investigation, resources, formal analysis, writing, conceptualization. SH: investigation, statistical analysis, draft editing, review. AVO: project administration, supervision, validation, conceptualization, methodology, validation. All authors read and approved the final manuscript.

Authors' information

Nima Hashemi: First Author, M.Sc. of Structural Engineering, Department of Civil and Environmental Engineering, Shahid Rajaee Teacher Training University, Shabanlou St., Tehran, Iran, 16788-15811.

Sina Hassanpour: Corresponding Author, M.Sc. of Structural Engineering, Department of Civil and Environmental Engineering, Sharif University of Technology, Azadi Ave., Tehran, Iran, 11155-1639.

Asghar Vatani Oskoei: Third Author, Ph.D., Associate Professor of Structural Engineering, Department of Civil and Environmental Engineering, Shahid Rajaei Teacher Training University, Shabanlou St., Tehran, Iran, 16788-15811.

Funding

The authors have not received funding for conducting this research.

Availability of data and materials

Not applicable.

Declarations

Competing interests

The authors declare that they have no competing interests.

Author details

¹Department of Civil and Environmental Engineering, Shahid Rajaei Teacher Training University, Tehran, Iran. ²Department of Civil and Environmental Engineering, Sharif University of Technology, Azadi Ave., Tehran, Iran.

Received: 19 August 2021 Accepted: 21 January 2022

Published online: 29 March 2022

References

- ACI. (2003). "Guide for bond and development of Straight Reinforcing Bars in Tension", 80, American Concrete Institute.
- ACI Committee 355. (2011). Qualification of Post-installed Adhesive Anchors in Concrete (ACI 355.4) and Commentary: An ACI Standard. American Concrete Institute.
- ACI Committee. (2014). Building code requirements for structural concrete (ACI 318-14) and commentary. American Concrete Institute.
- ACI 440.2R-08. (2008). Guide for the Design and Construction of Externally Bonded FRP Systems for Strengthening Concrete Structures, American Concrete Institute, Farmington Hills.
- Ahmad, A., & Raza, A. (2020). Reliability analysis of strength models for CFRP-confined concrete cylinders. *Composite Structures*, 244, 112312.
- Ahmad, S., Pilakoutas, K., & Neocleous, K. (2015). Stress-strain model for low-strength concrete in Uni-axial compression. *Arabian Journal for Science and Engineering*, 40(2), 313–328.
- Aslam, H. M. U., Sami, A., & Raza, A. (2021). Axial compressive behavior of damaged steel and GFRP bars reinforced concrete columns retrofitted with CFRP laminates. *Composite Structures*, 258, 113206.
- ASTM C39/C39M-14a, Standard Test Method for Compressive Strength of Cylindrical Concrete Specimens.
- Çalışkan, Ö., Yılmaz, S., Kaplan, H., & Kırac, N. (2013). Shear strength of epoxy anchors embedded into low strength concrete. *Construction and Building Materials*, 38, 723–730.
- Comert, M., Goksu, C. and Ilki, A., 2009, July. Towards a tailored stress-strain, behavior for FRP confined low strength concrete. In Proceedings of the 9th International Symposium on Fiber Reinforced Polymer Reinforcement for Concrete Structures, Sydney, Australia (pp. 13–15).
- Cook, R. A. (1993). Behavior of chemically bonded anchors. *Journal of Structural Engineering*, 119(9), 2744–2762.
- De Luca, A., & Nanni, A. (2011). Single-parameter methodology for the prediction of the stress-strain behavior of FRP-confined RC square columns. *Journal of Composites for Construction*, 15(3), 384–392.
- Durrani, A. J., Elnashai, A. S., Hashash, Y., Kim, S. J. & Masud, A., 2005. The Kashmir earthquake of October 8, 2005: A quick look report. MAE Center CD Release 05–04.
- Eligehausen, R., Mallé, R., & Silva, J. F. (2006). *Anchorage in concrete construction* (Vol. 10). New Jersey: Wiley.
- Erdil, B., Akyuz, U. & Yaman, I. O. (2008). Behaviour of CFRP reinforced low-strength concretes subjected to temperature changes and sustained loads. In: *The 14th World Conference on Earthquake Engineering, Beijing, China*.
- González, F., Fernández, J., Agronati, G., & Villanueva, P. (2018). Influence of construction conditions on strength of post installed bonded anchors. *Construction and Building Materials*, 165, 272–283.
- Hassan, A. F., Ali, M. H., & Sulaiman, H. T. (2016). Experimental study of CFRP confined low strength RC columns under concentric loads. *ZANCO Journal of Pure and Applied Sciences*, 28(4), 103–112.
- Ilki, A., Kumbasar, N. & Koc, V. (2002). Strength and deformability of low strength concrete confined by carbon fiber composite sheets. In *Proc. ASCE 15th Engineering Mechanics Conference*.
- Ilki, A., Kumbasar, N., & Koc, V. (2004). Low strength concrete members externally confined with FRP sheets. *Structural Engineering and Mechanics*, 18(2), 167–194.
- Ismail, R., Rashid, R. S., Chan, W. C., Jaafar, M. S., & Hejazi, F. (2019). Compressive behavior of concrete cylinder fully and partially confined by carbon fibre-reinforced polymer (CFRP). *Construction and Building Materials*, 201, 196–206.
- Khaloo, A., Tabatabaeian, M. and Khaloo, H. (2020). The axial and lateral behavior of low strength concrete confined by GFRP wraps: an experimental investigation. In *Structures* (Vol. 27, pp. 747–766). Elsevier.
- Lam, L., & Teng, J. G. (2003). Design-oriented stress-strain model for FRP-confined concrete. *Construction and Building Materials*, 17(6–7), 471–489.
- Lam, L., & Teng, J. G. (2004). Ultimate condition of fiber reinforced polymer-confined concrete. *Journal of Composites for Construction*, 8(6), 539–548.
- Lim, J. C., & Ozbakkaloglu, T. (2015). Influence of concrete age on stress-strain behavior of FRP-confined normal-and high-strength concrete. *Construction and Building Materials*, 82, 61–70.
- Mirmiran, A., & Shahawy, M. (1997). Behavior of concrete columns confined by fiber composites. *Journal of Structural Engineering*, 123(5), 583–590.
- Mosallam, A. (2004). Composites: construction materials for the new era. In: *Advanced polymer composites for structural applications in construction* (pp. 45–58). Woodhead Publishing.
- Najafi, B., & Khalaj and Sarand F.B., (2015). *The effect of nail angle in the nail pull strength with 3D numerical modeling*. University of technology of Qom.
- Nanni, A., & Bradford, N. M. (1995). FRP jacketed concrete under uniaxial compression. *Construction and Building Materials*, 9(2), 115–124.
- Naseer, A., Ali, S.M. and Hussain, Z. (2006). Reconnaissance report on the 8th October, 2005 earthquake Pakistan. Earthquake Engineering Centre, Department of Civil Engineering NWFU UET Peshawar, Pakistan.
- Nisikawa, T., Nakano, Y., Tsuchiya, Y., Sanada, Y. and Sameshima, H. (2005). *Quick report of damage investigation on buildings and houses due to October 8, 2005 Pakistan earthquake*. Japan Society of Civil Engineers (JSCE) and Architectural Institute of Japan (AIJ).
- Peiris, N., Rossetto, T., Burton, P., & Mahmood, S. (2006). *EEFIT mission: October 8, 2005 Kashmir earthquake*. Published Report.
- Pham, T. M., & Hadi, M. N. (2014a). Predicting stress and strain of FRP-confined square/rectangular columns using artificial neural networks. *Journal of Composites for Construction*, 18(6), 04014019.
- Pham, T. M., & Hadi, M. N. (2014b). Stress prediction model for FRP confined rectangular concrete columns with rounded corners. *Journal of Composites for Construction*, 18(1), 04013019.
- Pham, T. M., Hadi, M. N., & Youssef, J. (2015). Optimized FRP wrapping schemes for circular concrete columns under axial compression. *Journal of Composites for Construction*, 19(6), 04015015.
- Pour, A. F., Ozbakkaloglu, T., & Vincent, T. (2018). Simplified design-oriented axial stress-strain model for FRP-confined normal-and high-strength concrete. *Engineering Structures*, 175, 501–516.
- Raza, A., Rafique, U., Masood, B., Ali, B., ul Haq, F. & Nawaz, M.A. (2021). Performance evaluation of hybrid fiber reinforced low strength concrete cylinders confined with CFRP wraps. In *Structures* (vol. 31, pp. 182–189). Elsevier.
- Richart, F. E., Brandtæg, A., & Brown, R. L. (1928). *A study of the failure of concrete under combined compressive stresses*. University of Illinois at Urbana Champaign, College of Engineering.
- Saafi, M., Toutanji, H., & Li, Z. (1999). Behavior of concrete columns confined with fiber reinforced polymer tubes. *Materials Journal*, 96(4), 500–509.
- Saeed, H. Z., Khan, H. A., & Farooq, R. (2016). Experimental investigation of stress-strain behavior of CFRP confined Low Strength Concrete (LSC) cylinders. *Construction and Building Materials*, 104, 208–215.

- St, L., & Wold, S. (1989). Analysis of variance (ANOVA). *Chemometrics and Intelligent Laboratory Systems*, 6(4), 259–272.
- Taniguchi, H., Yasojima, A., & Araki, H. (2008). Seismic performance of reinforced concrete beams with low strength concrete. In *The 14th world conference on earthquake engineering*, China Scientific Book Services Co., Beijing, China.
- Teng, J. G., Jiang, T., Lam, L., & Luo, Y. Z. (2009). Refinement of a design-oriented stress–strain model for FRP-confined concrete. *Journal of Composites for Construction*, 13(4), 269–278.
- Upadhyaya, P., & Kumar, S. (2015). Pull-out capacity of adhesive anchors: An analytical solution. *International Journal of Adhesion and Adhesives*, 60, 54–62.
- Wu, Y. F., & Zhou, Y. W. (2010). Unified strength model based on Hoek-Brown failure criterion for circular and square concrete columns confined by FRP. *Journal of Composites for Construction*, 14(2), 175–184.
- Zhai, K., Fang, H., Guo, C., Fu, B., Ni, P., Ma, H., He, H., & Wang, F. (2021). Mechanical properties of CFRP-strengthened prestressed concrete cylinder pipe based on multi-field coupling. *Thin-Walled Structures*, 162, 107629.

Publisher's Note

Springer Nature remains neutral with regard to jurisdictional claims in published maps and institutional affiliations.

Submit your manuscript to a SpringerOpen[®] journal and benefit from:

- ▶ Convenient online submission
- ▶ Rigorous peer review
- ▶ Open access: articles freely available online
- ▶ High visibility within the field
- ▶ Retaining the copyright to your article

Submit your next manuscript at ▶ [springeropen.com](https://www.springeropen.com)
